frontiers in Pharmacology

ORIGINAL RESEARCH
published: 27 November 2018
doi: 10.3389/fphar.2018.01378

Necrostatin-1 Attenuates Trauma-Induced Mouse Osteoarthritis and IL-1β Induced Apoptosis via HMGB1/TLR4/SDF-1 in Primary Mouse Chondrocytes

Shuang Liang[1], Zheng-tao Lv[1,2], Jia-ming Zhang[1], Yu-ting Wang[1], Yong-hui Dong[3], Zheng-gang Wang[1], Kun Chen[1,3], Peng Cheng[1], Qing Yang[1], Feng-jing Guo[1], Wei-wei Lu[1], Wen-tao Zhu[1] and An-min Chen[1]**

[1] Department of Orthopedics, Tongji Hospital, Tongji Medical College, Huazhong University of Science & Technology, Wuhan, China, [2] Department of Oral Medicine, Infection and Immunity, Harvard School of Dental Medicine, Boston, MA, United States, [3] Department of Orthopaedic Surgery, Henan Provincial People's Hospital, Zhengzhou, China

OPEN ACCESS

Edited by:
Per-Johan Jakobsson,
Karolinska Institutet (KI), Sweden

Reviewed by:
Marina Korotkova,
Karolinska Institutet (KI), Sweden
Soon Yew Tang,
University of Pennsylvania,
United States

***Correspondence:**
Wen-tao Zhu
wentao-zhu@hotmail.com
An-min Chen
anminchen@hust.edu.cn

Specialty section:
This article was submitted to Inflammation Pharmacology, a section of the journal Frontiers in Pharmacology

Received: 15 August 2018
Accepted: 09 November 2018
Published: 27 November 2018

Citation:
Liang S, Lv Z-t, Zhang J-m, Wang Y-t, Dong Y-h, Wang Z-g, Chen K, Cheng P, Yang Q, Guo F-j, Lu W-w, Zhu W-t and Chen A-m (2018) Necrostatin-1 Attenuates Trauma-Induced Mouse Osteoarthritis and IL-1β Induced Apoptosis via HMGB1/TLR4/SDF-1 in Primary Mouse Chondrocytes. Front. Pharmacol. 9:1378. doi: 10.3389/fphar.2018.01378

Necrostatin-1 (Nec-1) is a specific small molecule inhibitor of receptor-interacting protein kinase 1 (RIPK1) that specifically inhibits phosphorylation of RIPK1. RIPK1 regulates inflammation and cell death by interacting with receptor-interacting serine/threonine protein kinases 3(RIPK3). We hypothesized that Nec-1 may have anti-inflammatory efficacy in patients with osteoarthritis (OA), as the pathophysiology of OA involves the activation of inflammation-related signaling pathways and apoptosis. In this study, we explored the effects of Nec-1 on interleukin (IL)-1β-induced inflammation in mouse chondrocytes and the destabilised medial meniscus (DMM) mouse model. Inhibiting RIPK1 with Nec-1 dramatically suppressed catabolism both *in vivo* and *in vitro*, but did not inhibit changes in subchondral bone. Nec-1 abolished the *in vitro* increases in matrix metalloproteinase (MMP) and ADAM metallopeptidase with thrombospondin type 1 motif 5 (ADAMTs5) expression induced by IL-1β. However, adding high-mobility group box 1 (HMGB1) partially abrogated this effect, indicating the essential role of HMGB1 and Nec-1 in the protection of primary chondrocytes. Furthermore, Nec-1 decreased the expression of Toll-like receptor 4 (TLR4) and stromal cell-derived factor-1 (SDF-1), and attenuated the interaction between TLR4 and HMGB1. Western blot results suggested that Nec-1 significantly suppressed IL-1β-induced NF-κB transcriptional activity, but not MAPK pathway. Micro-computed tomography, immunohistochemical staining, and Safranin O/Fast Green staining were used *in vivo* to assess the degree of destruction of OA cartilage. The results show that NEC-1 can significantly reduce the degree of destruction of OA cartilage. Therefore, Nec-1 may be a novel therapeutic candidate to treat OA.

Keywords: necrostatin-1, osteoarthritis, chondrocyte, necroptosis, apoptosis, inflammation

INTRODUCTION

Osteoarthritis (OA) is a common, age-related, degenerative disease characterized by the loss of articular cartilage integrity in the joint area, with varying degrees of articular osteophyte formation, subchondral bone remodeling, and synovitis (Glyn-Jones et al., 2015). The main risk factors for OA are age, gender, heredity, joint injuries, and obesity (Prieto-Alhambra et al., 2014). As one of the most common joint diseases, OA affects more than 9.5% of men and 18% of women aged >60 years (Woolf and Pfleger, 2003). It mainly arises in the hands, knees, hips and spine and is characterized by joint pain and loss of function (Dieppe and Lohmander, 2005). At present, treatments for OA are related to structural modifications and improving symptoms, including arthroscopic surgery, autologous cartilage transplantation, micro-fracture, and pharmaceutical drugs. However, the socioeconomic burden of treating OA is steadily rising, reaching 1% of the gross domestic product in developed countries (Hiligsmann et al., 2013).

Receptor interacting serine/threonine kinase 1 (RIPK1), a protein that regulates cell death and inflammation, is ubiquitously expressed in the ovaries, lungs, liver, intestines, limbs, and 25 other tissues (Yue et al., 2014). RIPK1 regulates apoptosis and necroptosis via kinase-dependent and -independent functions, which are essential for cell fate and inflammation (Dannappel et al., 2014; Rickard et al., 2014). Based on the RIP homotypic interaction motifs of RIPK1 and TIR-domain-containing adapter-inducing interferon (TRIF), Toll-like receptor (TLR)3, and TLR4 can also indirectly recruit RIPK1 through TRIF (Zhao et al., 2014). RIPK1 is located downstream of the tumour necrosis factor receptor (TNFR)1 and directly binds to the death domain in TNFR1 (Cook et al., 2014). Micheau et al. (Micheau and Tschopp, 2003; Meylan et al., 2004) showed that TNFR1 recruits RIPK1, adaptor TRADD, adaptor protein TRAF2, and ubiquitin ligases cIAP1 and cIAP2 to form complex I, which activates the mitogen-activated protein kinases (MAPK) signaling pathway and the transcription factor nuclear factor-kappaB (NF-κB) signaling pathway. After forming complex I, TRADD, TRAF2, and RIPK1 associate with FADD and caspase-8, constituting complex II and inducing apoptosis (Micheau and Tschopp, 2003). When caspases are inhibited by the pan-caspase inhibitor zVAD.fmk, necroptosis is executed by RIPK1 and/or RIPK3 (Newton, 2015).

Necrostatin-1 (Nec-1) is a specific small molecule inhibitor of RIPK1 that specifically inhibits phosphorylation of RIPK1 and RIPK1-mediated necroptosis and apoptosis (Degterev et al., 2005). Numerous studies have demonstrated that Nec-1 protects against various disease models *in vivo* and *in vitro*. In the ischaemia-reperfusion injury model after lung transplantation, Nec-1 reduces necroptosis and attenuates ischaemia-reperfusion lung injury by inhibiting the expression of RIPK1/RIPK3/MLKL (Kanou et al., 2018). In the cisplatin-induced nephrotoxicity mouse model, Nec-1 decreases apoptosis as well as proinflammatory cytokines and oxidative stress by inhibiting the activation of the NF-κB signaling pathway (Ning et al., 2018). Based on these results, we hypothesized that Nec-1 would have an anti-inflammatory effect on IL1β-induced chondrocytes and would reduce cartilage loss in a mouse model of OA. Consistent with our assumptions, Nec-1 had a significant protective effect on knee OA in mice. We also explored the specific mechanisms of this drug, including inflammation, apoptosis, and necroptosis.

MATERIALS AND METHODS

Reagents and Antibodies

Nec-1 was purchased from Selleck Chemicals (Houston, TX, United States). Nec-1 was dissolved in DMSO for *in vitro* use, and was dissolved in 5% DMSO, 45% PEG300 and ddH_2O, in turn. Recombinant murine IL-1β (#211-11B) was obtained from PeproTech (Rocky Hill, NJ, United States). Cell Counting Kit-8 (CCK-8), mouse antibody anti-GAPDH (BM3876), and secondary antibodies were purchased from Boster (Wuhan, China). Antibodies against RIPK1 (#3493), p-ERK (#4370), p-p38 (#4511), p-JNK (#9255), p-IkBa (#2859), p-p65 (#3033) and cleaved caspase-3 (#9964) were purchased from Cell Signaling Technology (Beverly, MA, United States). Rabbit antibodies against ERK (16443-1-AP), p38 (14064-1-AP), JNK (24164-1-AP), IkBa (10268-1-AP), p65 (10745-1-AP), matrix metalloproteinase (MMP)3 (17873-1-AP), TLR4 (19811-1-AP), HMGB1 (10829-1-AP), and stromal cell-derived factor-1 (SDF-1) (17402-1-AP) were purchased from Proteintech Group (Wuhan, Hubei, China). Antibodies against p-MLKL (ab196436), ADAMTs5 (ab41037) and MMP13 (ab39012) were obtained from Abcam (Cambridge, United Kingdom). Mouse SDF-1a/CXCL12 ELISA Kit was purchased from Bangyi (Shanghai, China).

Animals and the OA Model

Twelve-week-old male C57BL/6 mice (Experimental Animal Centre of Tongji Hospital, Wuhan, China), were housed in a light- and temperature-controlled room and fed a standard diet. The body weight of animals was presented in the **Supplementary Table I**. The destabilised medial meniscus (DMM) surgical model of OA was produced on the right knee according to a previously published protocol (Glasson et al., 2007). This animal experiment was approved by the Ethics Committee on Animal Experimentation of Tongji Medical College. Forty mice were divided into four groups (n = 10 per group): (1) sham group: sham-operated mice administered 15 μL vehicle (5% DMSO, 45% PEG300, and ddH_2O), (2) the sham + Nec-1 group: sham-operated mice treated with 15 μL Nec-1 (0.0468 mg/Kg), (3) the DMM group: DMM surgery mice administered 15 μL vehicle, and (4) the DMM + Nec-1 group: DMM surgery mice administered 15 μL Nec-1. The Nec-1 solution or vehicle was injected intra-articularly twice weekly for 8 weeks before sacrifice.

Micro-Computed Tomography (μ-CT) Imaging

The right knee joint structure was analyzed with a μ-CT system (μ-CT Scanco Medical, Bassersdorf, Switzerland). Images were obtained at 100 kV and 98 μA, with the resolution set to 10.5 μm. The three-dimensional images were reconstructed using the software built into the μ-CT system. Bone volume/tissue volume (BV/TV), trabecular thickness (Tb.Th.), trabecular number

(Tb.N.) and trabecular separation (Tb.Sp.) were analyzed using the μ-CT system.

Histological Staining and Analysis

After the animals were euthanised, right knee joint samples were fixed in 4% paraformaldehyde for 48 h, decalcified with 10% EDTA solution for 2 weeks, and embedded in paraffin wax. The knee joints were cut to a 4-μm thickness in the sagittal plane. Ten consecutive sections out of 25 were selected to represent the weight-bearing area of the femur and tibia, respectively, and were selected for scoring and quantifying IHC. The structure of the knee joints was observed under Safranin O/Fast Green staining, and the severity of OA changes was assessed using the Osteoarthritis Research Society International (OARSI) histopathology scoring system (Glasson et al., 2010). The DAB Histostain-SP kit was used for immunohistochemistry. Sections were incubated with specific antibodies to observe expression changes in MMP3, MMP13, and ADAMTs5. The number of positively stained cells was counted in the articular cartilage under a digital microscope (Nikon ECLIPSE Ti-S, Nikon, Tokyo, Japan).

Cell Culture

Mouse primary chondrocytes were collected from the knee cartilage of new-born C57BL/6 mice as described previously (Li et al., 2018). Articular cartilage derived from the knee joints was dissected into pieces in sterilized phosphate-buffered saline (PBS) and digested with 0.25% trypsin at 37°C for 30 min. The pieces were collected and incubated with 0.25% collagenase II at 37°C for 6 h. The primary chondrocytes were resuspended and cultured in DMEM/F12 with 10% foetal bovine serum (FBS), 100 U/mL penicillin and 100 mg/mL streptomycin sulfate in 25 cm^2 flasks at 37°C under 5% CO_2. Chondrocytes that had been passaged one or two times were used for the experiments.

Cell Viability Assay

The CCK-8 assay (Boster) was used to assess cell proliferation and viability. Briefly, primary chondrocytes were seeded at a density of 10,000 cells per well in 96-well plates. The next day, culture medium containing DMSO (vehicle) or an equal volume of Nec-1 (30 μmol/L) was added every day. The culture medium was replaced after 24, 48, and 72 h with 100 μL of medium containing a 10% CCK-8 solution, then incubated for 1 h in the dark at 37°C. Absorbance was measured at 450 nm with an ELX800 microplate reader (Bio-Tek, Winooski, VT, United States).

Apoptosis Analysis

An Annexin V-FITC/propidium iodide (PI) kit was used to detect apoptosis in chondrocytes in the presence of IL-1β (5 ng/mL) with or without Nec-1 (30 μmol/L). The chondrocytes were collected after treatment, washed three times in ice-cold PBS and resuspended in binding buffer. Then, 5 μL PI and 5 μL Annexin V were added to the buffer for 15 min at 4°C in the dark. A FACS Calibur flow cytometer (BD, Franklin Lakes, NJ, United States) was used to analyze the apoptotic cells in the early and late phases according to the manufacturer's instructions.

Immunofluorescence

Primary chondrocytes were fixed in 4% paraformaldehyde for 15 min at room temperature, permeabilised with 0.1% Triton X-100 for 5 min and blocked with 0.1% bovine serum albumin for 30 min. The cells were incubated with primary antibody against HMGB1 overnight at 4°C, followed by goat anti-rabbit IgG/Cy3 (Invitrogen, Camarillo, CA, United States) as a second antibody for 1 h at room temperature. Finally, 4,6-diamidino-2-phenylindole (DAPI) was added to the cells to stain the nuclei in the dark. Immunofluorescence was imaged with a fluorescence microscope (Evos Flauto; Life Technologies, Carlsbad, CA, United States).

Co-immunoprecipitation and Western Blotting

IgG and Protein A+G agarose were added to the cell lysates for 2 h to block non-specific binding. A primary antibody was added to the mixture with shaking overnight at 4°C, followed by another incubation with Protein A+G agarose for 3 h. After centrifugation, the Protein A+G agarose was washed five times with lysis buffer, resuspended in sodium dodecyl sulfate sample buffer and boiled for 10 min. The BCA assay (Boster) was used to measure the concentration of protein in the samples used for western blotting. Equivalent quantities of samples were subjected to sodium dodecyl sulfate-polyacrylamide gel electrophoresis and then transferred to polyvinylidene fluoride membranes (Millipore, Billerica, MA, United States). After incubation with primary antibodies overnight at 4°C on a shaker, the membranes were incubated with secondary antibodies and then scanned with the ChemiDocTM XRS C System (Bio-Rad Laboratories, Hercules, CA, United States).

Statistical Analysis

All experiments were independently performed at least three times with similar results. The results are presented as the mean ± standard deviation. Student's *t*-test was used to assess differences between two groups, and one-way analysis of variance (ANOVA) followed by Dunnett's *post hoc* test was used to compare groups. *P*-values < 0.05 were considered significant.

RESULTS

Nec-1 Attenuates Cartilage Degeneration *in vivo*

We confirmed a significant change in tibial and femoral cartilage in DMM mice compared with sham-operated mice. Specifically, Safranin O/Fast Green staining demonstrated the structural changes, fibrillations, and vertical clefts of cartilage in the DMM mice (**Figure 1A**). MMP3, MMP13, and ADAMTs5 were expressed in articular cartilage according to the immunohistochemical staining (**Figures 1C,D**). Using the OARSI scores system, the degree of OA cartilage destruction in these four groups was quantified by three blinded observers (YW, JZ, and ZW). The OARSI scores (**Figure 1B**) were significantly lower (tibia: 2 points; femur: 2 points; $P < 0.05$) in the

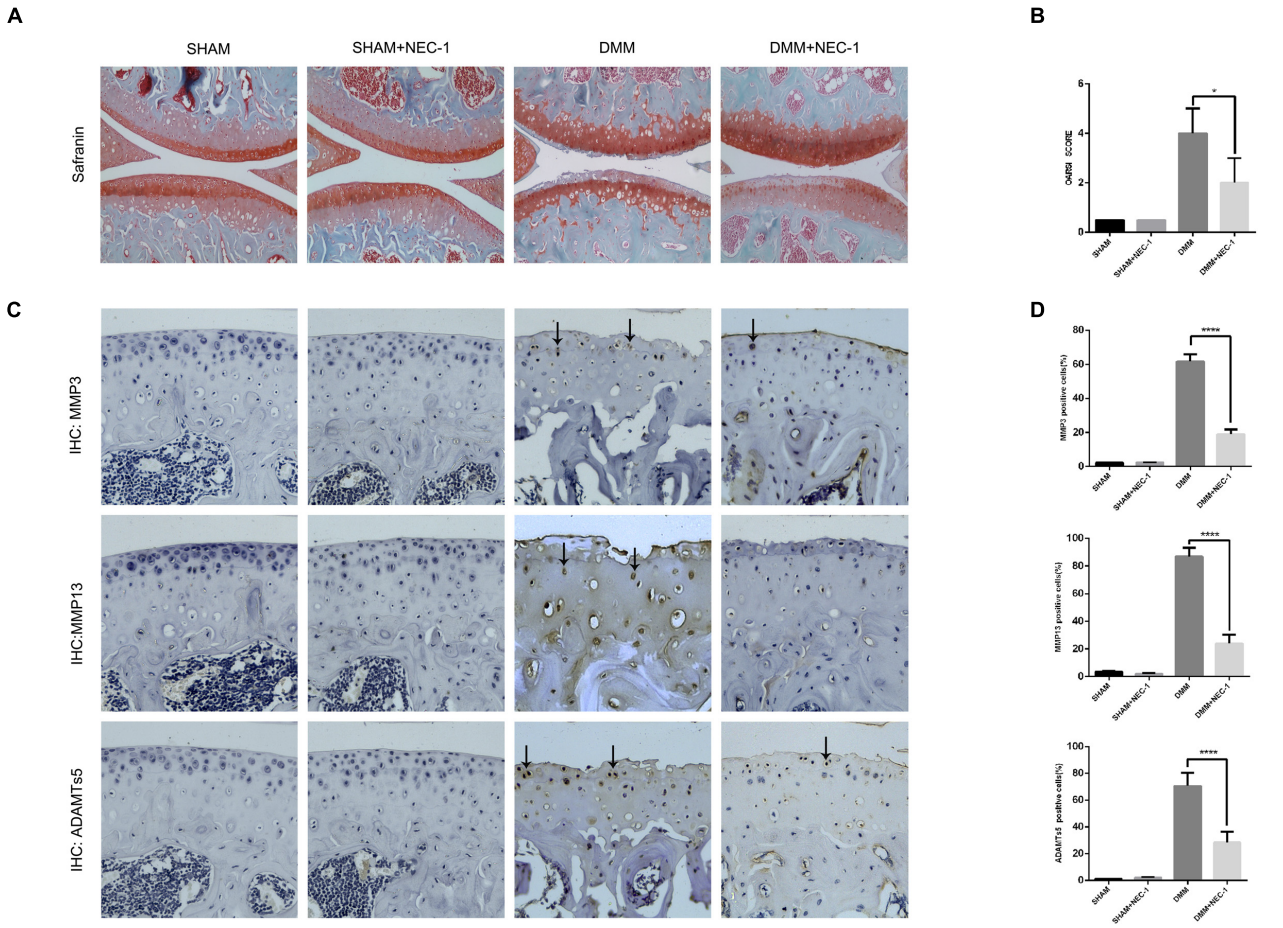

FIGURE 1 | Inhibition of RIPK1 with Nec-1 attenuates cartilage degeneration. **(A)** Safranin O/Fast Green staining in the sagittal plane of tibial and femoral cartilage from the sham, sham + Nec-1, destabilised medial meniscus (DMM), and the DMM + Nec-1 groups (n = 10). Scale bar = 100 μm. **(B)** Osteoarthritis Research Society International (OARSI) histopathology scores of sham and DMM mice treated with vehicle and Nec-1, respectively. **(C)** Expression of MMPs and ADAMTs5 were determined by immunohistochemical staining of the cartilage from each group (n = 10). **(D)** MMPs and ADAMTs5 positive cells were quantified using Image-J software. *$P < 0.05$, ****$P < 0.0001$.

DMM + Nec-1-treated group than those in the DMM-treated mice (tibia: 4 points; femur: 4 points). No significant differences were found between the Sham + Nec-1-treated group and the sham controls ($P > 0.05$). These results indicate that Nec-1 attenuated the destruction of articular cartilage in DMM mice, and it had similar effects on decreasing the expression of MMP3, MMP13, and ADAMTs5 in articular cartilage compared to the sham group. The OARSI scores revealed the significant protective effect of Nec-1 against OA in mice.

Nec-1 Does Not Affect Tibial Subchondral Bone Remodeling

The effects of Nec-1 on the structure of tibial subchondral bone were measured and analyzed by μCT in the DMM OA mice. BV/TV, Tb.Th, and Tb.Sp increased significantly in the DMM group compared with the sham group, whereas Tb.N decreased (**Figures 2A,B**). However, no differences in BV/TV, Tb.Th, Tb.Sp, or Tb.N were observed between the DMM + Nec-1 and sham groups. These results indicate that Nec-1 does not affect tibial subchondral bone remodeling in mice with OA.

Nec-1 Inhibits IL-1β-Induced Catabolism *in vitro*

The CCK-8 assay was performed to measure the cytotoxic effects of Nec-1 on chondrocytes. As shown in **Figure 3A**, Nec-1(30 μmol/L) did not decrease cell viability or proliferation after 24, 48, or 72 h. MMPs and ADAMTs are key regulators of cartilage destruction (Mengshol et al., 2000; Liang et al., 2018). To determine the anti-inflammation significance of Nec-1 on IL-1 induced release of catabolic enzymes by chondrocytes, the cells were co-treated with Nec-1 in the presence or absence of IL-1β for 48 h. As shown in **Figures 3B,C**, the protein levels of MMP3, MMP13, and ADAMTs5 increased significantly after induction by IL-1β, but were significantly reversed by Nec-1 treatment in 48 and 72 h.

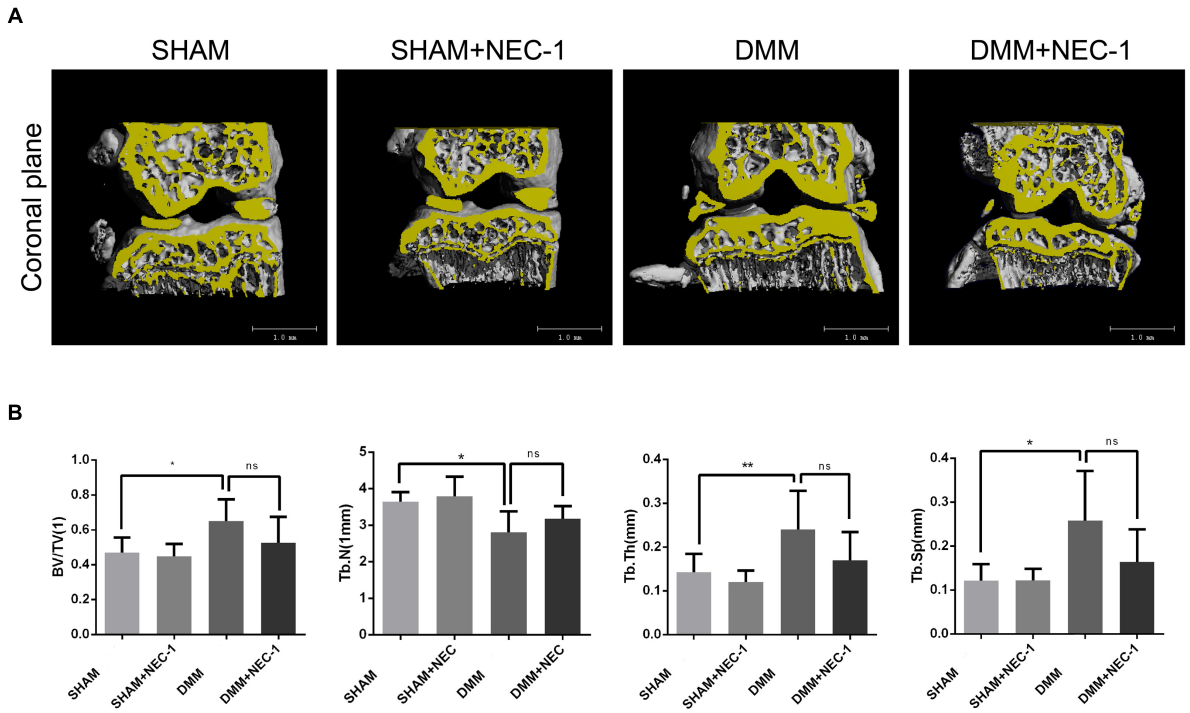

FIGURE 2 | Inhibition of RIPK1 with Nec-1 does not affect tibial subchondral bone remodeling. **(A)** Three-dimensional micro-computed tomography coronal views of the medial and lateral tibial subchondral bone from each group. **(B)** Histograms represent the trabecular structural analysis of tibia platform subchondral trabecular: trabecular bone volume/tissue volume (BV/TV), trabecular number (Tb.N), trabecular thickness (Tb.Th) and trabecular separation (Tb.Sp). Data are the mean ± SD. $n = 10$. DMM different from sham ($^*P < 0.05$, $^{**}P < 0.01$); ns: not significant.

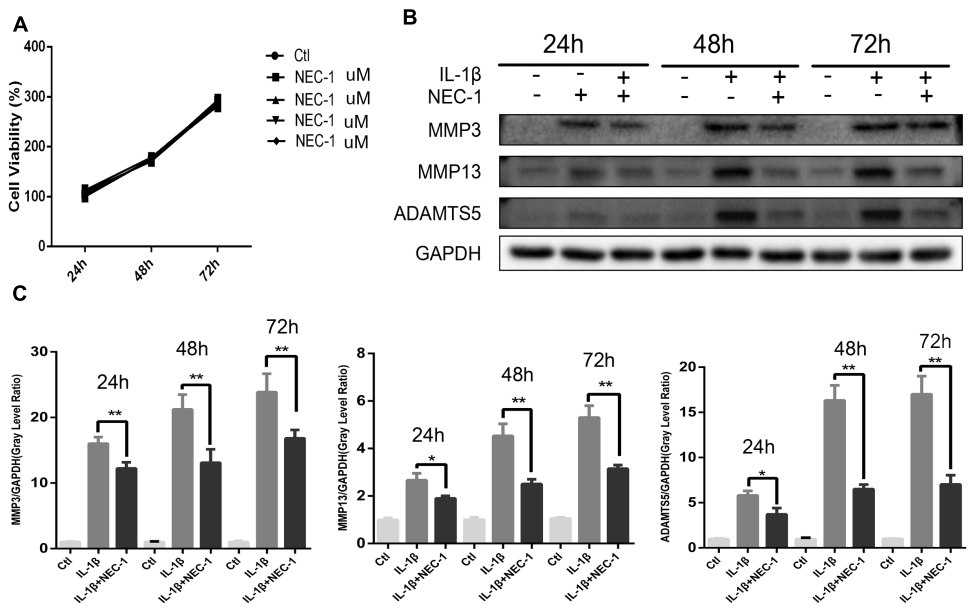

FIGURE 3 | Effects of Nec-1 on interleukin (IL)-1β-induced matrix metalloproteinase (MMP) and ADAM metallopeptidase with thrombospondin type 1 motif 5 (ADAMTS5) expression. Primary chondrocytes pretreated with Nec-1 (30 μmol/L) for 30 min were treated with IL-1β (5 ng/mL) for further 24, 48, and 72 h. **(A)** Cells were treated with Nec-1 (30 μmol/L) for 24, 48, and 72 h, and viability was evaluated by the Cell Counting Kit-8 (CCK-8) assay. **(B)** The protein levels of MMP-3, MMP-13, and ADAMTs5 were determined by western blot analysis. **(C)** Relative protein expression was quantified using ImageJ software. The experiments were repeated three times independently. $^*P < 0.05$, $^{**}P < 0.01$ vs. IL-1β group.

Nec-1 Prevents Chondrocyte Inflammation by RIPK1/HMGB1/TLR4 Signaling and Apoptosis but Not Necroptosis

HMGB1, a key mediator of inflammation, plays an important role in initiating OA and rheumatoid arthritis (Wang et al., 2015; Jiang et al., 2017). In our experiment, the HMGB1 expression level decreased significantly in the IL-1β + Nec-1 group compared to the IL-1β group (**Figures 4B,C**). The immunofluorescence analysis showed similar results. IL-1β promoted HMGB1 expression and translocation from the nucleus to the cytoplasm, and these effects were significantly inhibited by Nec-1 (**Figure 4A**). To determine the role of HMGB1 in attenuated inflammation, we treated chondrocytes with rHmgb1 (HMGBiotech, HM-115) and IL-1β. The results showed that the decreased expression of MMP3, MMP13, ADAMTs5, and SDF1 was abrogated by adding HMGB1 (**Figures 5A,B**). The tendency is consistent with the results of the cell experiments. As the interaction between HMGB1 and TLR4 is responsible for amplifying the inflammatory response, co-immunoprecipitation was performed with HMGB1 and TLR4 (**Figures 5D,E**). The results indicated that Nec-1 decreased the interaction between HMGB1 and TLR4 induced by IL-1β.

The levels of apoptosis and expression of cleaved caspase-3 were determined to investigate the role of apoptosis in the anti-inflammatory effects of Nec-1 in articular chondrocytes. The expression of cleaved caspase-3, the key major effector of caspases, was significantly augmented in IL-1β-induced chondrocytes, which was reversed by Nec-1 (**Figures 6C,D**). Correspondingly, apoptosis was detected by Annexin V-FITC/PI staining and the levels were lower in the IL-1β-Nec-1-combined treatment group (**Figures 6A,B**), in agreement with the changes in the amount of cleaved caspase-3. There were no differences in necroptosis marker P-MLKL in our experiment (**Figures 4B,C**). These results demonstrate that Nec-1 protects chondrocytes from inflammation by inhibiting RIPK1/HMGB1/TLR4 signaling and apoptosis, but not necroptosis.

Nec-1 Reduces Inflammatory Markers *in vivo*

The role of SDF-1in the pathogenesis of OA has attracted more attention in recent years. In our *in vivo* experiment, ELISA indicated serum SDF-1 expression in DMM mice and sham mice. The levels of serum SDF-1α decreased by 30.5% in DMM + Nec-1 group at 8 weeks post-surgery compared with DMM group; this difference was statistically significant (**Figure 5C**). The tendency is consistent with the results of the cell experiments. The effects of Nec-1 on the expression of HMGB1 and TLR4 in the cartilage were also validated by ICH in the mouse model (**Figures 5F,G**). The results showed that Nec-1 significantly decreased the expression of HMGB1 and TLR4 in the cartilage of DMM + Nec-1 group compared with DMM group.

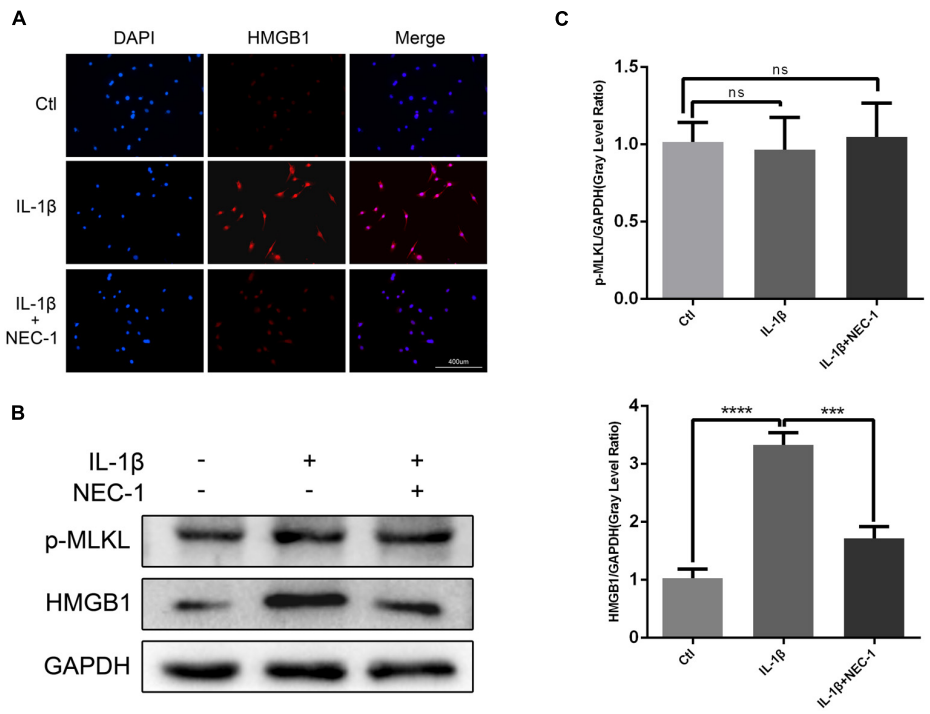

FIGURE 4 | Nec-1 acts through high-mobility group box 1 (HMGB1) to regulate chondrocytes. **(A)** The subcellular location of HMGB1 was determined by immunofluorescence staining for endogenous HMGB1 (red) and DAPI for nuclei (blue). Bar = 400 μm. **(B)** The protein levels of HMGB1 and p-MLKL were determined by western blot analysis. **(C)** Relative protein expression was quantified using ImageJ software. The experiments were repeated three times independently. ***$P < 0.0006$, ****$P < 0.0001$.

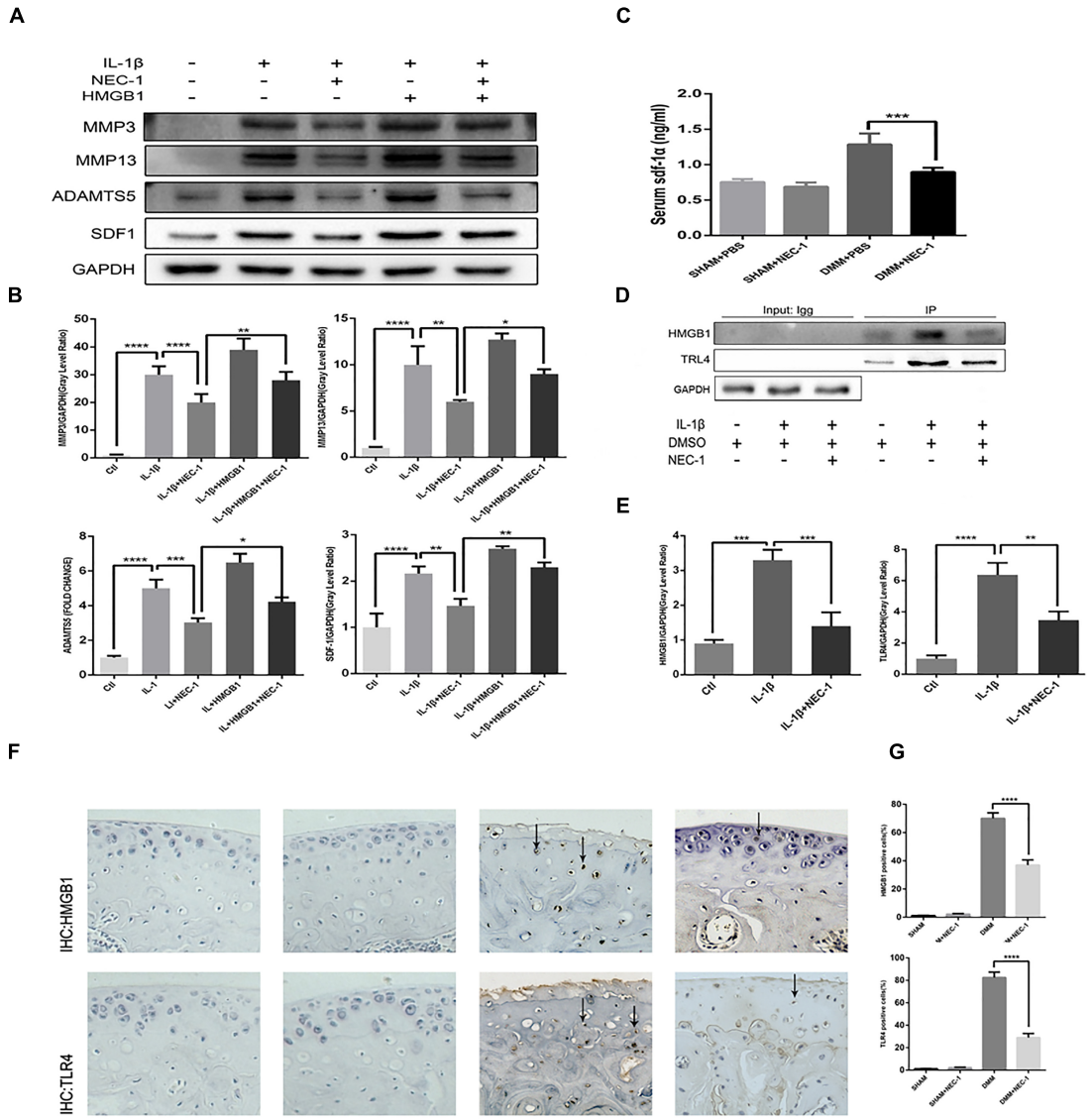

FIGURE 5 | The RIPK1/toll-like receptor 4 (TLR4) pathway attenuates chondrocyte degeneration induced by Nec-1. **(A,B)** The expression levels of MMPs, ADAMTs5, and stromal cell-derived factor-1 (SDF1) in primary chondrocytes from the ctl, IL-1β, IL-1β + Nec-1, IL-1β + HMGB1, and IL-1β + HMGB1 + Nec-1 groups were determined by western blotting. **(C)** Serum levels of SDF-1α protein were measured by ELISA. Serum were collected from mice euthanized at 8 weeks post-DMM surgery (n = 10 for each group). **(D,E)** Interactions between HMGB1 and TLR4 were detected by co-immunoprecipitation. Relative protein expression was quantified using ImageJ software. The relative protein expression levels of HMGB1 and TLR4 were normalized to GAPDH and expressed as a relative value. **(F,G)** Expression of HMGB1 and TLR4 were determined by immunohistochemical staining of the cartilage from each group (n = 10). HMGB1 and TLR4 positive cells were quantified using Image-J software. The experiments were repeated three times independently. $^{*}P < 0.05$, $^{**}P < 0.01$, $^{***}P < 0.0006$, and $^{****}P < 0.0001$.

HNF-κB but Not MAPK Is Involved in the Protective Effect of Nec-1 in Chondrocytes

To investigate the exact mechanism of the protective effect of Nec-1 in articular chondrocytes, we checked the activation status of the NF-κB and MAPK pathways in chondrocytes induced by IL-1β combined with/without Nec-1 for 15 min. As shown in **Figure 7**, Nec-1 significantly inhibited the phosphorylation of IkBa and p65 (**Figures 7C,D**). No significant differences in the level of phosphorylation of the MAPK pathway were detected between the IL-1β + Nec-1 and control groups (**Figures 7A,B**).

DISCUSSION

osteoarthritis is the most common form of arthritis and involves multiple proinflammatory cytokines, including IL-1β, TNF, and IL-6. IL-1β is secreted by chondrocytes, mononuclear cells, osteoblasts, and synoviocytes. It suppresses the production of

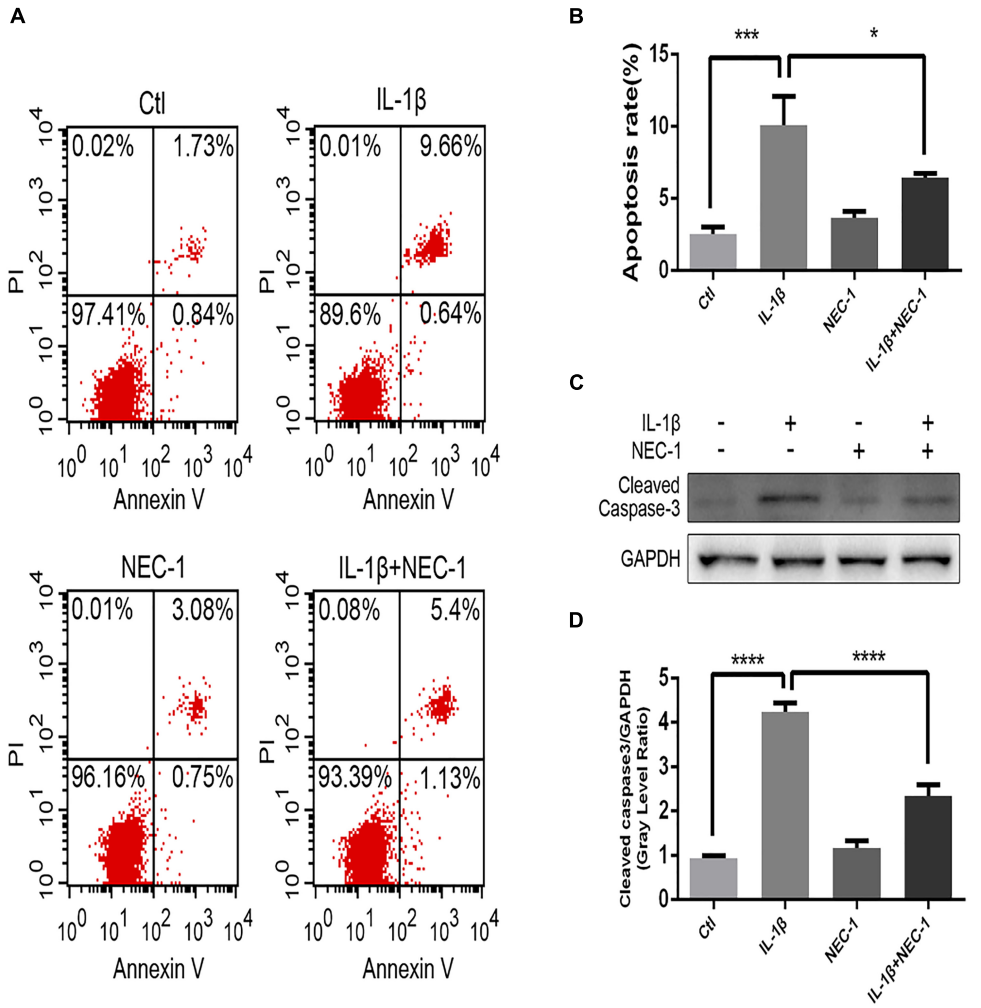

FIGURE 6 | Nec-1 protects against IL-1β-induced apoptosis. **(A)** Chondrocytes were stained with Annexin V-FITC/propidium iodide (PI) and detected by flow cytometry. **(B)** Histograms represent the rate of apoptosis. Ctl: 2.57%; IL-1β: 10.3%; Nec-1: 3.83%; IL-1β + Nec-1: 6.53%. **(C,D)** The cleaved caspase-3 protein level was determined by western blot analysis. The experiments were repeated three times independently. $^{*}P < 0.05$, $^{***}P < 0.0006$, and $^{****}P < 0.0001$.

collagen II and aggrecan and stimulates the release of MMP-3, MMP13, and ADAMTs5. MMPs and ADAMTs are key regulators of cartilage destruction (Lv et al., 2017). Nec-1 is a specific small molecule inhibitor of RIPK1 that specifically inhibits phosphorylation of RIPK1. Although numerous studies have demonstrated that Nec-1 attenuates various *in vivo* and *in vitro* disease models (Zhang et al., 2017), the effects of Nec-1 on mice with OA are unknown. Our study demonstrated that Nec-1 attenuated OA *in vivo* and *in vitro* through the RIPK1/HMGB1/TLR4 and apoptosis pathways. We constructed a destabilized OA animal model by transecting the anterior cruciate ligament of the right knee in mice. After 8 weeks of DMM, we observed significant destruction of articular cartilage and subchondral bone sclerosis in the operated knees.

HMGB1 is a member of the damage-associated molecular patterns (DAMPs) that is released from dead/damaged cells during inflammation, tissue injury, necrosis, and hypoxia (Srikrishna and Freeze, 2009), creating a sustained inflammatory niche. Immunohistochemistry results indicate that the expression of HMGB1 increases in a complete Freund's adjuvant-induced OA animal model (Li et al., 2016). TLR4, a member of the toll-like receptor family, activates the inflammatory response by interacting with DAMPs (Ooboshi and Shichita, 2016). A previous study demonstrated that HMGB1 is unable to aggravate the inflammatory response in TLR4 knockout mice (Nadatani et al., 2013). Duprez et al. (2011) showed that pretreatment with a RIPK1 inhibitor confers protection against systemic inflammatory response syndrome by reducing the expression of DAMPs. In the present study, we demonstrated that Nec-1 enhanced articular structural recovery by inhibiting the expression of HMGB1 and its interaction with TLR4. The effects of Nec-1 on the expression of HMGB1 and TLR4 in the articular cartilage were validated by ICH in the mouse model. We also explored the role of SDF-1α in the protection of Nec-1. SDF-1α is a catabolic factor that degrades cartilage by decreasing proteoglycan content and increasing MMP activities

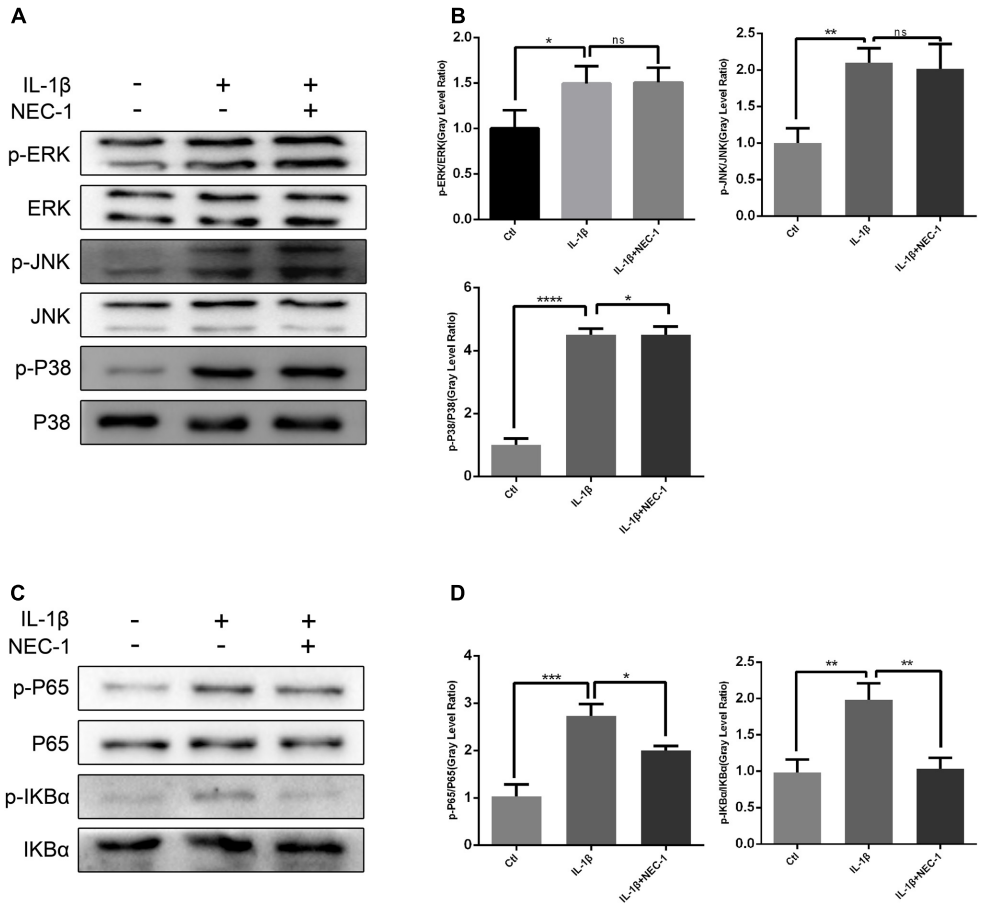

FIGURE 7 | Nec-1 represses activation of the NF-κB signaling pathway in chondrocytes induced by IL-1β. In order to reduce the levels of phosphorylated MAPK and NF-KB, the chondrocytes were serum-starved for 8 h. Since phosphorylated MAPK and NF-KB levels reach a maximum within 30 min and degrade within 1 h, the chondrocytes were treated with IL-1β for 15 min. **(A,B)** Nec-1 did not repress the MAPK signaling pathway. Chondrocytes were starved with DMEM in the absence of FBS for 8 h, and then pre-treated with or without Nec-1 (30 μmol/L) for 1 h. Subsequently, the chondrocytes were treated with IL-1β (5 ng/mL) for 15 min. **(C,D)** Nec-1 represses the NF-κB signaling pathway. The experiments were repeated three times independently. $^{*}P < 0.05$, $^{**}P < 0.01$, $^{***}P < 0.0006$, and $^{****}P < 0.0001$.

(Dong et al., 2016). We found that decreased expression of SDF1 was abrogated by adding HMGB1. Our *in vivo* experiment also demonstrated that the levels of serum SDF-1α obviously decreased in DMM + Nec-1 mice compared with DMM mice. Consistent with our findings, Yun et al. (2017) also showed that SDF-1α expression and release increased in HMGB1-stimulated eye inflammation in mice (Yun et al., 2017).

Apoptosis is a type of programmed, highly regulated cell death that includes chromosome condensation, DNA fragmentation, cell shrinkage, plasma membrane blebbing, and the formation of apoptotic bodies (Kerr et al., 1972). Numerous studies have revealed that apoptosis is highly correlated with the degree of cartilage destruction and matrix catabolism in OA tissues (Musumeci et al., 2015). Furthermore, the release of cellular contents and inflammatory mediators from apoptotic cells may play an additional role in aggravating OA (Hwang and Kim, 2015). Chondrocyte degradation and apoptosis may form a vicious cycle. Cleaved caspase-3, the most important executioner caspase, is a specific hallmark of apoptosis. Our *in vitro* study indicated that Nec-1 significantly inhibited apoptosis and inflammation in chondrocytes induced by IL-1β. Necroptosis is a novel mechanism of programmed necrosis that incorporates features of apoptosis and necrosis. Phosphorylation of MLKL by the autophosphorylation of RIPK3 during necroptosis results in the translocation of MLKL from the cytosol to the plasma membrane (Sun et al., 2012). However, our experiments showed that IL-1β was unable to induce necroptosis *in vitro*. A previous study showed that TNF-α and IFN-β cannot induce necroptosis in the absence of zVAD (McComb et al., 2014), which may account for our results.

Some studies have suggested that negative regulation of the NF-κB and MAPK signaling pathways controls RIPK1. NF-κB and MAPK are vital signaling pathways involved in the production of MMPs and the regulation of chondrocyte proliferation, apoptosis and differentiation. Our results show that Nec-1 inhibited the phosphorylation of IkB-α and p65, suggesting a possible underlying mechanism for the inhibitory effects of Nec-1 in OA. However, changes in the phosphorylation levels of

JNK, ERK and p38 were not significant, and were inconsistent with previous studies (Kemeny et al., 1988; Kim and Lee, 2017).

As the most important proinflammatory cytokine, IL-1β contributes to the pathogenesis of OA through several mechanisms including downregulation of anabolic events and upregulation of catabolic and inflammatory responses (Kapoor et al., 2011). Nowadays, IL-1β stimulation (2–20 ng/ml) is used as a conventional *in vitro* model to recapitulate the pathological condition of DMM OA model (Wang et al., 2017; Hu et al., 2018; Tan et al., 2018). Yasuhito (Song et al., 2018) and Shinsuke (Kihara et al., 2017) have demonstrated that IL-1β-positive chondrocytes increased significantly in DMM mice compared with levels observed in sham mice. It is well known that estrogen plays an important role in the progression of OA (Ma et al., 2007; Tanamas et al., 2011). OA is more prevalent in men than women before age 50. In order to rule out the effects of estrogen in mice model, only male mice were chosen in our experiments. The DMM mouse model used in our study is advantageous as it results in mild OA and is more sensitive to the effects of treatment, compared with other destabilized OA animal models. This DMM model better simulates the disease modifications of aged spontaneous mouse models of OA (Glasson et al., 2007). In other cell line experiments, the dosage of Nec-1 used in cell culture models was 10 to 300 μM (Zheng et al., 2014; Chen et al., 2015; Suzuki et al., 2015; Wu et al., 2015), and 1.65–30 mg/kg in animal models (Najjar et al., 2016; Ning et al., 2018). In our study, the dosage of Nec-1 used in animal was 0.0468 mg/Kg body weight, and 30 μM in cell culture models. In conclusion, Nec-1 had a protective effect against the destabilized OA animal model and chondrocyte inflammation. This protective effect was attributed to inhibiting apoptosis, HMGB1 expression, and the NF-κB signaling pathway. Furthermore, the mechanisms associated with HMGB1 included interactions with TLR4 and the suppression of SDF1. However, further studies are needed to investigate other Nec-1 targets and the details of the role of RIPK1 in the pathology of OA.

AUTHOR CONTRIBUTIONS

A-mC and W-tZ designed the experiments and revised the manuscript. SL conducted the experiments and prepared the manuscript. Z-tL and J-mZ analyzed the data. Y-tW, Z-gW, KC, W-wL, and PC contributed to clarifying and supervising the writing of the manuscript. F-jG and QY helped with manuscript revision. All authors have read and approved the final manuscript.

FUNDING

This study was sponsored by grants from the National Natural Science Foundation of China (Grant Nos. 81672168 and 81472082 to A-mC and Grant No. 81601951 to QY) and the Natural Science Foundation of Hubei Province of China (2018CFB714 to W-tZ).

SUPPLEMENTARY MATERIAL

The Supplementary Material for this article can be found online at: https://www.frontiersin.org/articles/10.3389/fphar.2018.01378/full#supplementary-material

REFERENCES

Chen, G., Cheng, X., Zhao, M., Lin, S., Lu, J., Kang, J., et al. (2015). RIP1-dependent BID cleavage mediates TNFalpha-induced but Caspase-3-independent cell death in L929 fibroblastoma cells. *Apoptosis* 20, 92–109. doi: 10.1007/s10495-014-1058-0

Cook, W. D., Moujalled, D. M., Ralph, T. J., Lock, P., Young, S. N., Murphy, J. M., et al. (2014). RIPK1- and RIPK3-induced cell death mode is determined by target availability. *Cell Death Differ.* 21, 1600–1612. doi: 10.1038/cdd.2014.70

Dannappel, M., Vlantis, K., Kumari, S., Polykratis, A., Kim, C., Wachsmuth, L., et al. (2014). RIPK1 maintains epithelial homeostasis by inhibiting apoptosis and necroptosis. *Nature* 513, 90–94. doi: 10.1038/nature13608

Degterev, A., Huang, Z., Boyce, M., Li, Y., Jagtap, P., Mizushima, N., et al. (2005). Chemical inhibitor of nonapoptotic cell death with therapeutic potential for ischemic brain injury. *Nat. Chem. Biol.* 1, 112–119. doi: 10.1038/nchembio711

Dieppe, P. A., and Lohmander, L. S. (2005). Pathogenesis and management of pain in osteoarthritis. *Lancet* 365, 965–973. doi: 10.1016/S0140-6736(05)71086-2

Dong, Y., Liu, H., Zhang, X., Xu, F., Qin, L., Cheng, P., et al. (2016). Inhibition of SDF-1alpha/CXCR4 signalling in subchondral bone attenuates post-traumatic osteoarthritis. *Int. J. Mol. Sci.* 17:E943. doi: 10.3390/ijms17060943

Duprez, L., Takahashi, N., Van Hauwermeiren, F., Vandendriessche, B., Goossens, V., Vanden, B. T., et al. (2011). RIP kinase-dependent necrosis drives lethal systemic inflammatory response syndrome. *Immunity* 35, 908–918. doi: 10.1016/j.immuni.2011.09.020

Glasson, S. S., Blanchet, T. J., and Morris, E. A. (2007). The surgical destabilization of the medial meniscus (DMM) model of osteoarthritis in the 129/SvEv mouse. *Osteoarthritis Cartilage* 15, 1061–1069. doi: 10.1016/j.joca.2007.03.006

Glasson, S. S., Chambers, M. G., Van Den Berg, W. B., and Little, C. B. (2010). The OARSI histopathology initiative - recommendations for histological assessments of osteoarthritis in the mouse. *Osteoarthritis Cartilage* 18(Suppl. 3), S17–S23. doi: 10.1016/j.joca.2010.05.025

Glyn-Jones, S., Palmer, A. J., Agricola, R., Price, A. J., Vincent, T. L., Weinans, H., et al. (2015). Osteoarthritis. *Lancet* 386, 376–387. doi: 10.1016/S0140-6736(14)60802-3

Hiligsmann, M., Cooper, C., Arden, N., Boers, M., Branco, J. C., Luisa, B. M., et al. (2013). Health economics in the field of osteoarthritis: an expert's consensus paper from the European society for clinical and economic aspects of osteoporosis and osteoarthritis (ESCEO). *Semin. Arthritis Rheum.* 43, 303–313. doi: 10.1016/j.semarthrit.2013.07.003

Hu, X., Ji, X., Yang, M., Fan, S., Wang, J., Lu, M., et al. (2018). Cdc42 is essential for both articular cartilage degeneration and subchondral bone deterioration in experimental osteoarthritis. *J. Bone Miner. Res.* 33, 945–958. doi: 10.1002/jbmr.3380

Hwang, H. S., and Kim, H. A. (2015). Chondrocyte apoptosis in the pathogenesis of osteoarthritis. *Int. J. Mol. Sci.* 16, 26035–26054. doi: 10.3390/ijms161125943

Jiang, Y., Zhu, L., Zhang, T., Lu, H., Wang, C., Xue, B., et al. (2017). BRD4 has dual effects on the HMGB1 and NF-kappaB signalling pathways and is a potential therapeutic target for osteoarthritis. *Biochim. Biophys. Acta* 1863, 3001–3015. doi: 10.1016/j.bbadis.2017.08.009

Kanou, T., Ohsumi, A., Kim, H., Chen, M., Bai, X., Guan, Z., et al. (2018). Inhibition of regulated necrosis attenuates receptor-interacting protein kinase 1-mediated ischemia-reperfusion injury after lung transplantation. *J. Heart Lung Transpl.* 37, 1261–1270. doi: 10.1016/j.healun.2018.04.005

Kapoor, M., Martel-Pelletier, J., Lajeunesse, D., Pelletier, J. P., and Fahmi, H. (2011). Role of proinflammatory cytokines in the pathophysiology of osteoarthritis. *Nat. Rev. Rheumatol.* 7, 33–42. doi: 10.1038/nrrheum.2010.196

Kemeny, E., Fillit, H. M., Damle, S., Mahabir, R., Kefalides, N. A., Gregory, J. D., et al. (1988). Monoclonal antibodies to heparan sulfate proteoglycan: development and application to the study of normal tissue and pathologic human kidney biopsies. *Connect. Tissue Res.* 18, 9–25.

Kerr, J. F., Wyllie, A. H., and Currie, A. R. (1972). Apoptosis: a basic biological phenomenon with wide-ranging implications in tissue kinetics. *Br. J. Cancer* 26, 239–257.

Kihara, S., Hayashi, S., Hashimoto, S., Kanzaki, N., Takayama, K., Matsumoto, T., et al. (2017). Cyclin-dependent Kinase inhibitor-1-deficient mice are susceptible to osteoarthritis associated with enhanced inflammation. *J. Bone Miner. Res.* 32, 991–1001. doi: 10.1002/jbmr.3080

Kim, S. J., and Lee, S. M. (2017). Necrostatin-1 protects against D-Galactosamine and lipopolysaccharide-induced hepatic injury by preventing TLR4 and RAGE signaling. *Inflammation* 40, 1912–1923. doi: 10.1007/s10753-017-0632-3

Li, C., Cai, H., Meng, Q., Feng, Y., Guo, H., Fang, W., et al. (2016). IL-1beta mediating high mobility group box protein-1 expression in condylar chondrocyte during temporomandibular joint inflammation. *J. Oral Pathol. Med.* 45, 539–545. doi: 10.1111/jop.12401

Li, K., Zhang, Y., Zhang, Y., Jiang, W., Shen, J., Xu, S., et al. (2018). Tyrosine kinase Fyn promotes osteoarthritis by activating the beta-catenin pathway. *Ann. Rheum. Dis.* 77, 935–943. doi: 10.1136/annrheumdis-2017-212658

Liang, S., Zhang, J. M., Lv, Z. T., Cheng, P., Zhu, W. T., and Chen, A. M. (2018). Identification of Skt11-regulated genes in chondrocytes by integrated bioinformatics analysis. *Gene* 677, 340–348. doi: 10.1016/j.gene.2018.08.013

Lv, Z. T., Liang, S., Huang, X. J., Cheng, P., Zhu, W. T., and Chen, A. M. (2017). Association between ADAM12 single-nucleotide polymorphisms and knee osteoarthritis: a meta-analysis. *Biomed. Res. Int.* 2017:5398181. doi: 10.1155/2017/5398181

Ma, H. L., Blanchet, T. J., Peluso, D., Hopkins, B., Morris, E. A., and Glasson, S. S. (2007). Osteoarthritis severity is sex dependent in a surgical mouse model. *Osteoarthritis Cartilage* 15, 695–700. doi: 10.1016/j.joca.2006.11.005

McComb, S., Cessford, E., Alturki, N. A., Joseph, J., Shutinoski, B., Startek, J. B., et al. (2014). Type-I interferon signaling through ISGF3 complex is required for sustained Rip3 activation and necroptosis in macrophages. *Proc. Natl. Acad. Sci. U.S.A.* 111, E3206–E3213. doi: 10.1073/pnas.1407068111

Mengshol, J. A., Vincenti, M. P., Coon, C. I., Barchowsky, A., and Brinckerhoff, C. E. (2000). Interleukin-1 induction of collagenase 3 (matrix metalloproteinase 13) gene expression in chondrocytes requires p38, c-Jun N-terminal kinase, and nuclear factor kappaB: differential regulation of collagenase 1 and collagenase 3. *Arthritis Rheum.* 43, 801–811. doi: 10.1002/1529-0131(200004)43:4801::AID-ANR103.0.CO2-4

Meylan, E., Burns, K., Hofmann, K., Blancheteau, V., Martinon, F., Kelliher, M., et al. (2004). RIP1 is an essential mediator of Toll-like receptor 3-induced NF-kappa B activation. *Nat. Immunol.* 5, 503–507. doi: 10.1038/ni1061

Micheau, O., and Tschopp, J. (2003). Induction of TNF receptor I-mediated apoptosis via two sequential signaling complexes. *Cell* 114, 181–190.

Musumeci, G., Aiello, F. C., Szychlinska, M. A., Di Rosa, M., Castrogiovanni, P., and Mobasheri, A. (2015). Osteoarthritis in the XXIst century: risk factors and behaviours that influence disease onset and progression. *Int. J. Mol. Sci.* 16, 6093–6112. doi: 10.3390/ijms16036093

Nadatani, Y., Watanabe, T., Tanigawa, T., Ohkawa, F., Takeda, S., Higashimori, A., et al. (2013). High-mobility group box 1 inhibits gastric ulcer healing through Toll-like receptor 4 and receptor for advanced glycation end products. *PLoS One* 8:e80130. doi: 10.1371/journal.pone.0080130

Najjar, M., Saleh, D., Zelic, M., Nogusa, S., Shah, S., Tai, A., et al. (2016). RIPK1 and RIPK3 kinases promote cell-death-independent inflammation by toll-like receptor 4. *Immunity* 45, 46–59. doi: 10.1016/j.immuni.2016.06.007

Newton, K. (2015). RIPK1 and RIPK3: critical regulators of inflammation and cell death. *Trends Cell Biol.* 25, 347–353. doi: 10.1016/j.tcb.2015.01.001

Ning, Y., Shi, Y., Chen, J., Song, N., Cai, J., Fang, Y., et al. (2018). Necrostatin-1 attenuates cisplatin-induced nephrotoxicity through suppression of apoptosis and oxidative stress and retains klotho expression. *Front. Pharmacol.* 9:384. doi: 10.3389/fphar.2018.00384

Ooboshi, H., and Shichita, T. (2016). [DAMPs (damage-associated molecular patterns) and inflammation]. *Nihon Rinsho* 74, 573–578.

Prieto-Alhambra, D., Judge, A., Javaid, M. K., Cooper, C., Diez-Perez, A., and Arden, N. K. (2014). Incidence and risk factors for clinically diagnosed knee, hip and hand osteoarthritis: influences of age, gender and osteoarthritis affecting other joints. *Ann. Rheum. Dis.* 73, 1659–1664. doi: 10.1136/annrheumdis-2013-203355

Rickard, J. A., O'Donnell, J. A., Evans, J. M., Lalaoui, N., Poh, A. R., Rogers, T., et al. (2014). RIPK1 regulates RIPK3-MLKL-driven systemic inflammation and emergency hematopoiesis. *Cell* 157, 1175–1188. doi: 10.1016/j.cell.2014.04.019

Song, J., Baek, I. J., Chun, C. H., and Jin, E. J. (2018). Dysregulation of the NUDT7-PGAM1 axis is responsible for chondrocyte death during osteoarthritis pathogenesis. *Nat. Commun.* 9:3427. doi: 10.1038/s41467-018-05787-0

Srikrishna, G., and Freeze, H. H. (2009). Endogenous damage-associated molecular pattern molecules at the crossroads of inflammation and cancer. *Neoplasia* 11, 615–628.

Sun, L., Wang, H., Wang, Z., He, S., Chen, S., Liao, D., et al. (2012). Mixed lineage kinase domain-like protein mediates necrosis signaling downstream of RIP3 kinase. *Cell* 148, 213–227. doi: 10.1016/j.cell.2011.11.031

Suzuki, T., Kikuguchi, C., Sharma, S., Sasaki, T., Tokumasu, M., Adachi, S., et al. (2015). CNOT3 suppression promotes necroptosis by stabilizing mRNAs for cell death-inducing proteins. *Sci. Rep.* 5:14779. doi: 10.1038/srep14779

Tan, Q., Chen, B., Wang, Q., Xu, W., Wang, Y., Lin, Z., et al. (2018). A novel FGFR1-binding peptide attenuates the degeneration of articular cartilage in adult mice. *Osteoarthritis Cartilage* doi: 10.1016/j.joca.2018.08.012 [Epub ahead of print].

Tanamas, S. K., Wijethilake, P., Wluka, A. E., Davies-Tuck, M. L., Urquhart, D. M., Wang, Y., et al. (2011). Sex hormones and structural changes in osteoarthritis: a systematic review. *Maturitas* 69, 141–156. doi: 10.1016/j.maturitas.2011.03.019

Wang, W. J., Yin, S. J., and Rong, R. Q. (2015). PKR and HMGB1 expression and function in rheumatoid arthritis. *Genet. Mol. Res.* 14, 17864–17870. doi: 10.4238/2015.December.22.11

Wang, Y., Yu, D., Liu, Z., Zhou, F., Dai, J., Wu, B., et al. (2017). Exosomes from embryonic mesenchymal stem cells alleviate osteoarthritis through balancing synthesis and degradation of cartilage extracellular matrix. *Stem Cell Res. Ther.* 8:189. doi: 10.1186/s13287-017-0632-0

Woolf, A. D., and Pfleger, B. (2003). Burden of major musculoskeletal conditions. *Bull. World Health Organ.* 81, 646–656.

Wu, P., Zhu, X., Jin, W., Hao, S., Liu, Q., and Zhang, L. (2015). Oxaliplatin triggers necrosis as well as apoptosis in gastric cancer SGC-7901 cells. *Biochem. Biophys. Res. Commun.* 460, 183–190. doi: 10.1016/j.bbrc.2015.03.003

Yue, F., Cheng, Y., Breschi, A., Vierstra, J., Wu, W., Ryba, T., et al. (2014). A comparative encyclopedia of DNA elements in the mouse genome. *Nature* 515, 355–364. doi: 10.1038/nature13992

Yun, J., Jiang, G., Wang, Y., Xiao, T., Zhao, Y., Sun, D., et al. (2017). The HMGB1-CXCL12 complex promotes inflammatory cell infiltration in uveitogenic T Cell-induced chronic experimental autoimmune uveitis. *Front. Immunol.* 8:142. doi: 10.3389/fimmu.2017.00142

Zhang, C., Lin, S., Li, T., Jiang, Y., Huang, Z., Wen, J., et al. (2017). Mechanical force-mediated pathological cartilage thinning is regulated by necroptosis and apoptosis. *Osteoarthritis Cartilage* 25, 1324–1334. doi: 10.1016/j.joca.2017.03.018

Zhao, C., Pavicic, P. J., Datta, S., Sun, D., Novotny, M., and Hamilton, T. A. (2014). Cellular stress amplifies TLR3/4-induced CXCL1/2 gene transcription in mononuclear phagocytes via RIPK1. *J. Immunol.* 193, 879–888. doi: 10.4049/jimmunol.1303396

Zheng, H. W., Chen, J., and Sha, S. H. (2014). Receptor-interacting protein kinases modulate noise-induced sensory hair cell death. *Cell Death Dis.* 5:e1262. doi: 10.1038/cddis.2014.177

Conflict of Interest Statement: The authors declare that the research was conducted in the absence of any commercial or financial relationships that could be construed as a potential conflict of interest.

Copyright © 2018 Liang, Lv, Zhang, Wang, Dong, Wang, Chen, Cheng, Yang, Guo, Lu, Zhu and Chen. This is an open-access article distributed under the terms of the Creative Commons Attribution License (CC BY). The use, distribution or reproduction in other forums is permitted, provided the original author(s) and the copyright owner(s) are credited and that the original publication in this journal is cited, in accordance with accepted academic practice. No use, distribution or reproduction is permitted which does not comply with these terms.